Figure S1: Location of proxies within the surface temperature dataset (D_{surf}). A) SST proxies with time intervals indicated as followed: black circles, all three-time intervals represented. Red circles: PETM ± latest Paleocene intervals; orange circles, EECO interval (b) Terrestrial sites with time intervals indicated as in (a) and green circles, LP only. Sites are shown on the paleomagnetic reference frame.

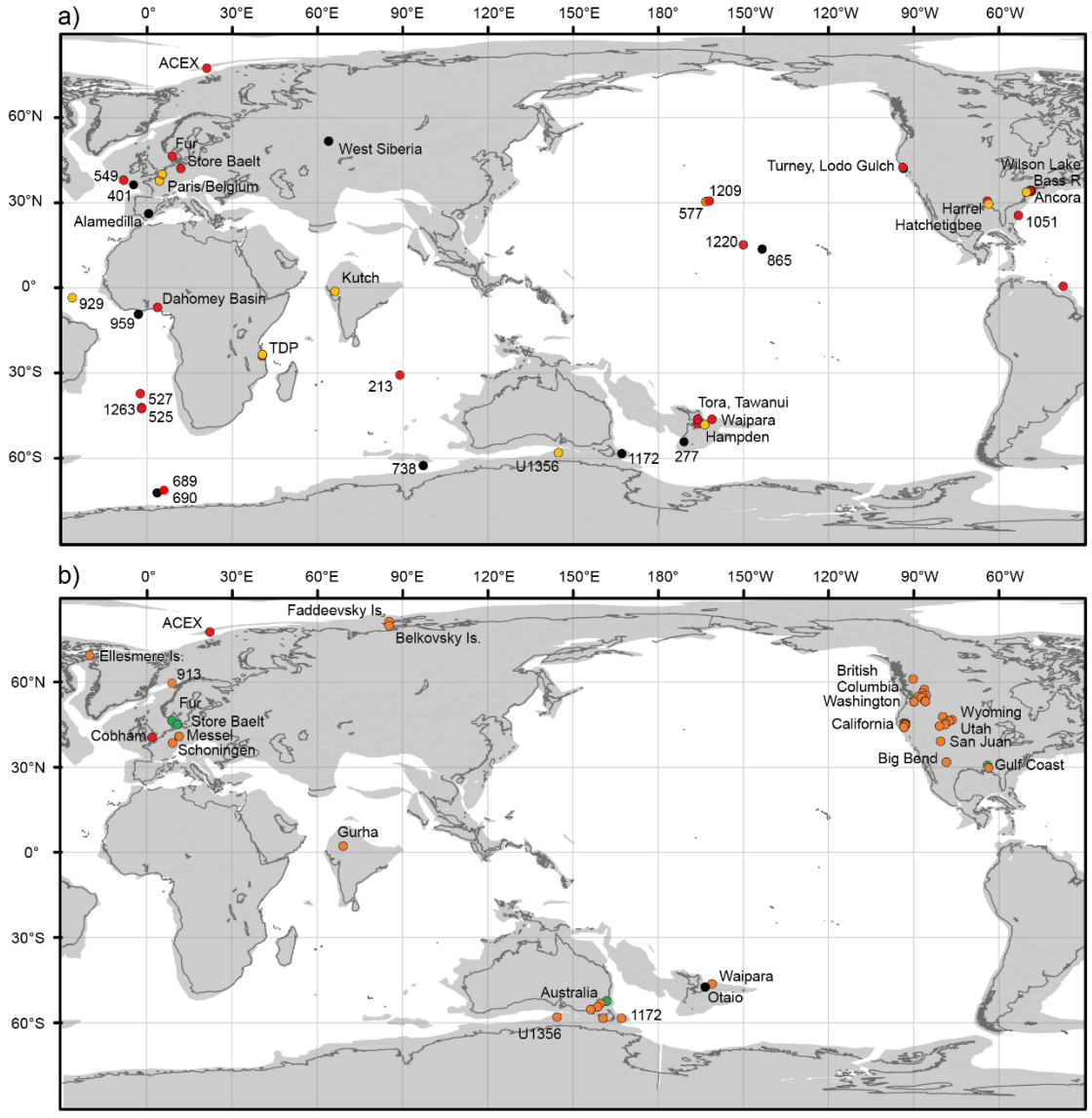

Figure S2: Predicted surface warming by Gaussian process regression (i.e. D_{surf}-*3*) and associated uncertainties. Anomalies are relative to the present-day zonal mean surface temperature. Circles indicate all available SST and LAT proxy data for the respective time slice that were used to train the model. Circles for locations where multiple proxy reconstructions are available are slightly shifted in latitude for improved visibility

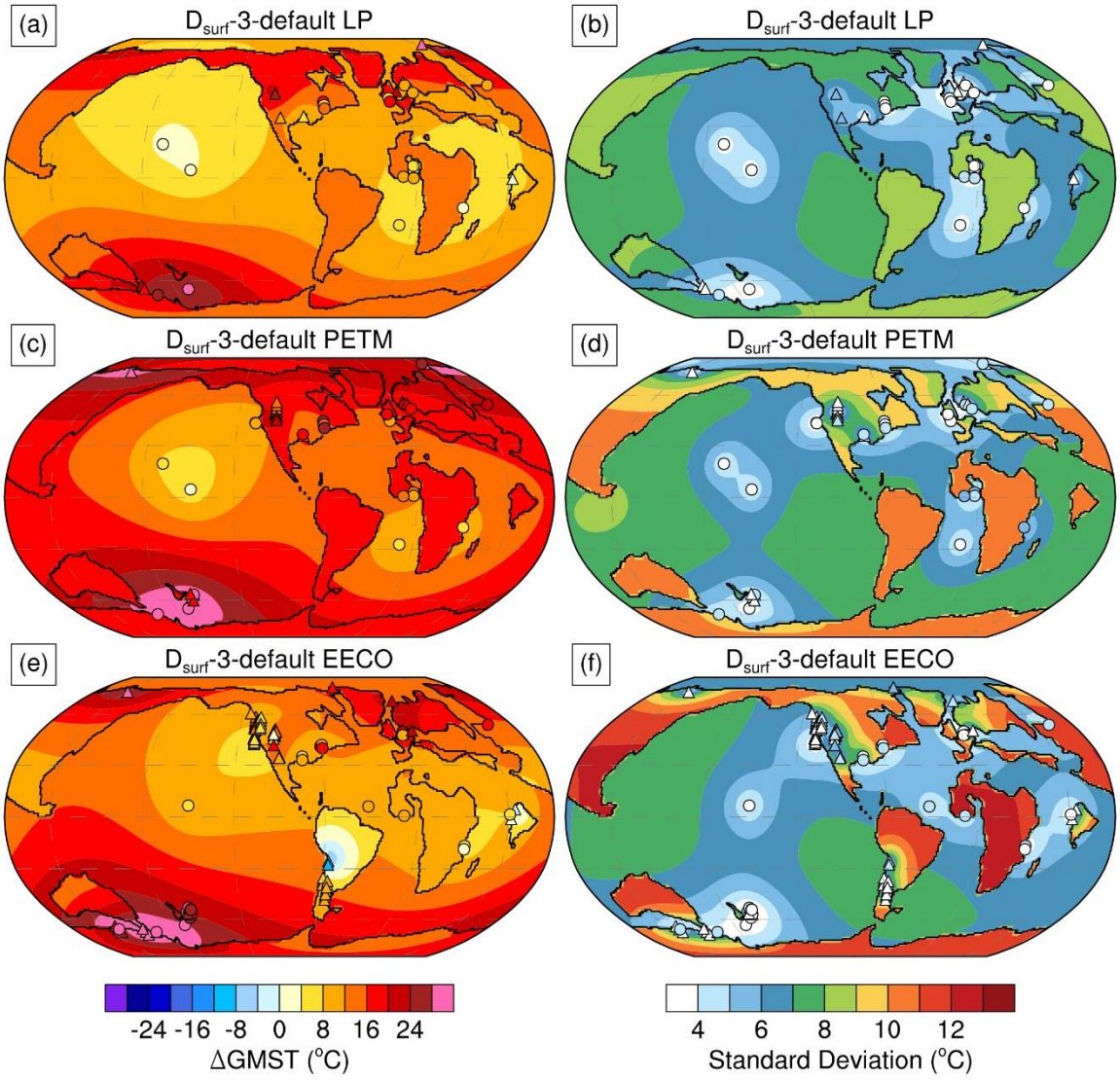

Figure S3: Illustration of D_{surf}-4 comparing zonal-mean near-surface air temperature at sea level, averaged over all months between 1981 and 2000, from ERA5 reanalysis (solid) and Eq. 3 (dashed).

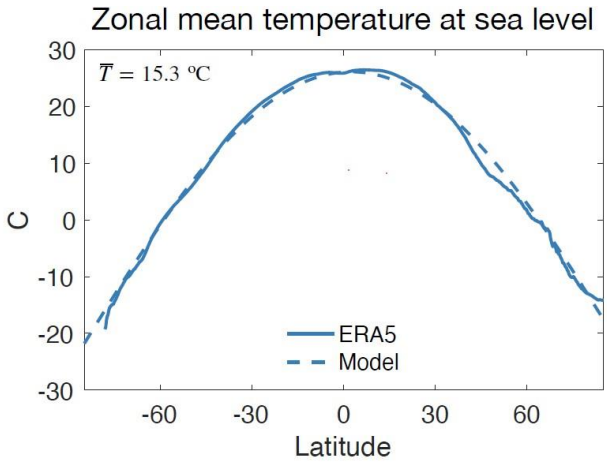

Figure S4: Illustration of D_{surf}-4 illustrating the average (red line) and 90% confidence interval (red shading) of zonal-mean temperatures computing from proxy LAT (purple) and SST (green) data from the EECO (left), LP (center), and PETM (right).

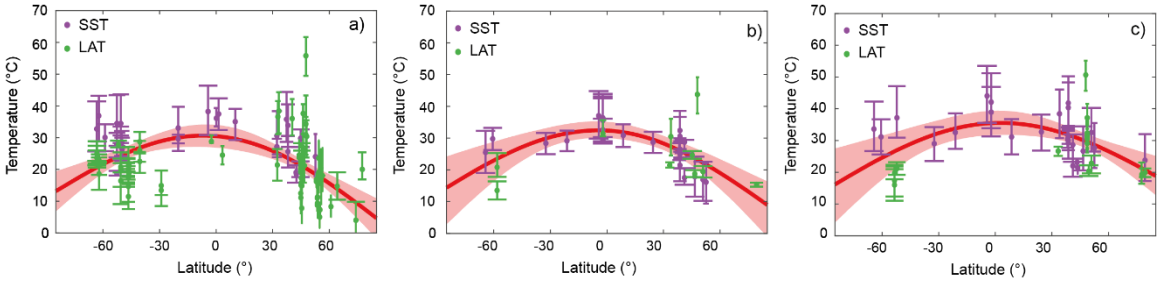

Figure S5: (a) A simple model of the shape of the latitudinal gradient. The relationship between surface temperature and latitude is linear between 50-80° and described by a second order polynomial between 0-50°. Endmember models depict the shape of the latitudinal temperature gradient at each of the four corners of panel B (TL = top left, etc.). **(b)** Contours show the extent to which D_{comb} underestimates GMST in °C, based on the algebraic model illustrated in (a). This indicates that D_{comb} will underestimate GMST by 0.6-1.5°C, depending on the latitudinal temperature gradient and the degree to which this gradient departs from a straight line, but not on absolute temperature. The positions of the CESM1 simulations EO3 and EO4 are based on matching the zonal average latitudinal gradient of those simulations to the model shown in (a). **(c)** EO3 hemispheric latitudinal gradients and algebraic model matched to these profiles. Shaded areas indicate the approximate regions from which the DeepMIP proxy data are taken for the calculations presented in the main text. The difference between the true simulation GMST and that calculated using the D_{comb} method is given, assuming deep water formation takes place at a location with a temperature equal to that of the mean of all data >65°N/S. **(d)** As in (c), but for the EO4 simulation.

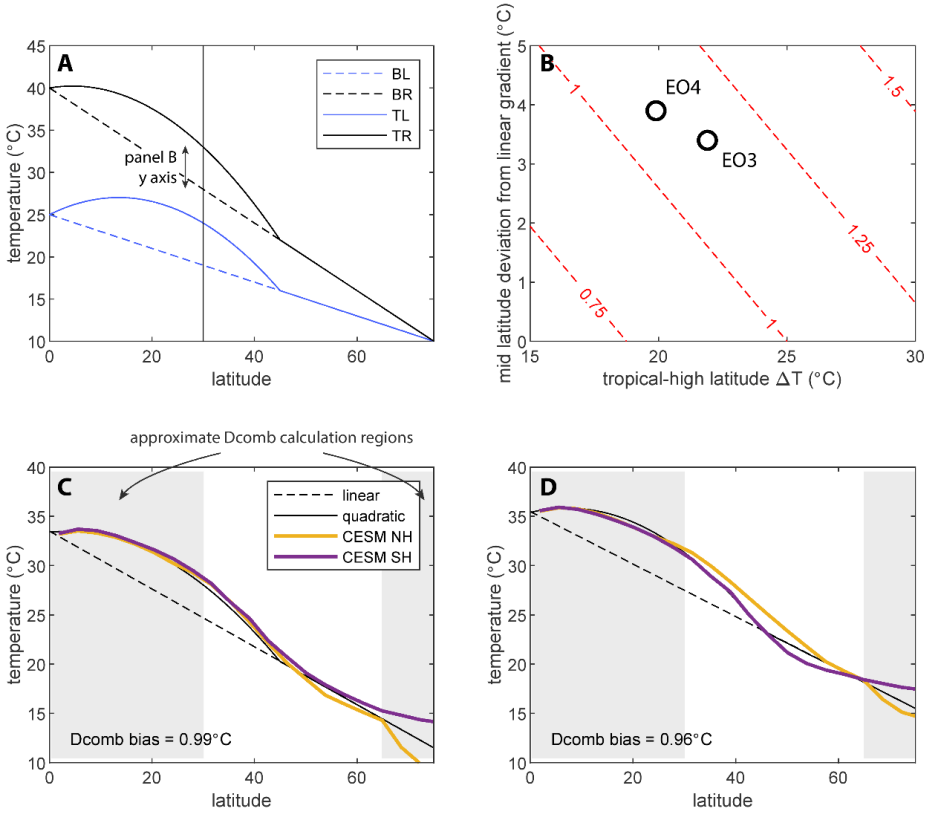

Figure S6: Predicted surface warming by Gaussian process regression using *D_{surf}-3* for the EECO for the five core experiments (see Table 2). Anomalies are relative to the present-day zonal mean surface temperature. Circles indicate all available SST and LAT proxy data for the respective time slice and experiment that were used to train the model. Circles for locations where multiple proxy reconstructions are available are slightly shifted in latitude for improved visibility.

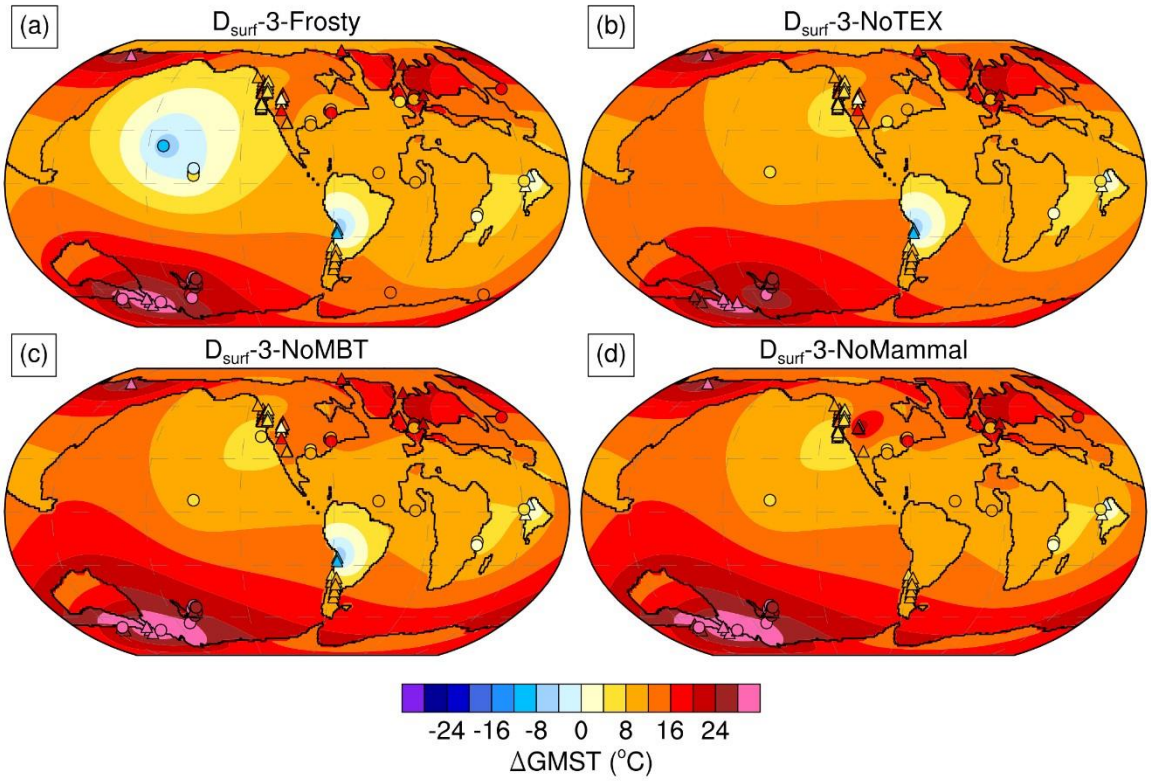

Figure S7: Predicted surface warming by Gaussian process regression using *D_{surf}-3* for the PETM for the five core experiments (see Table 2). Anomalies are relative to the present-day zonal mean surface temperature. Circles indicate all available SST and LAT proxy data for the respective time slice and experiment that were used to train the model. Circles for locations where multiple proxy reconstructions are available are slightly shifted in latitude for improved visibility.

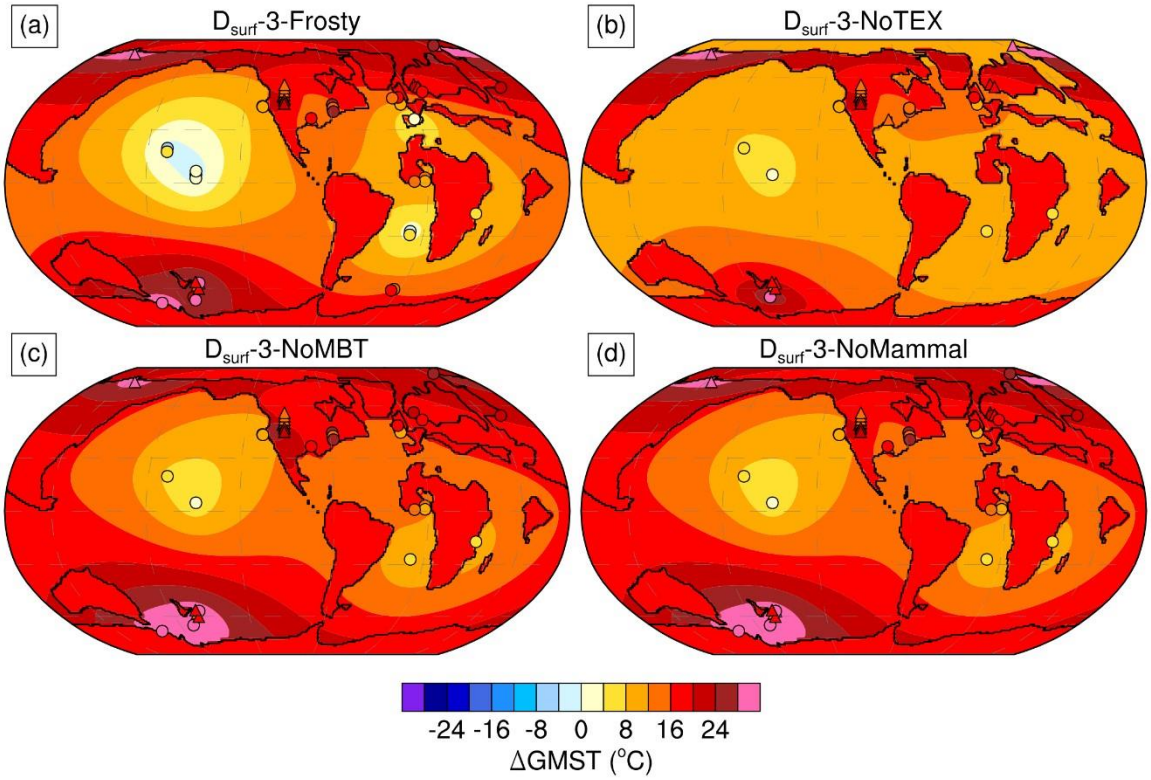

Figure S8: Predicted surface warming by Gaussian process regression using *D_{surf}-3* for the latest Paleocene for the five core experiments (see Table 2). Anomalies are relative to the present-day zonal mean surface temperature. Circles indicate all available SST and LAT proxy data for the respective time slice and experiment that were used to train the model. Circles for locations where multiple proxy reconstructions are available are slightly shifted in latitude for improved visibility.

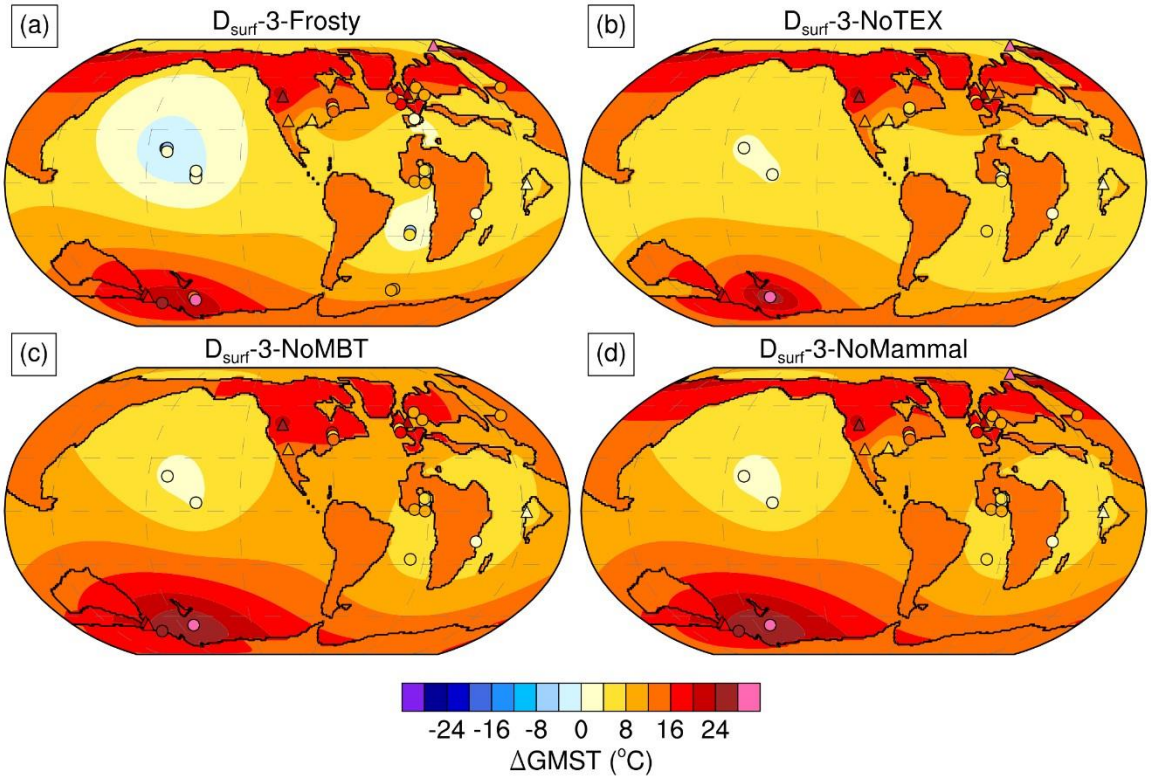

Figure S9: Sequential removal of one GMST method at a time (jackknife resampling) was performed to examine the influence of a single method upon the average GMST estimate.

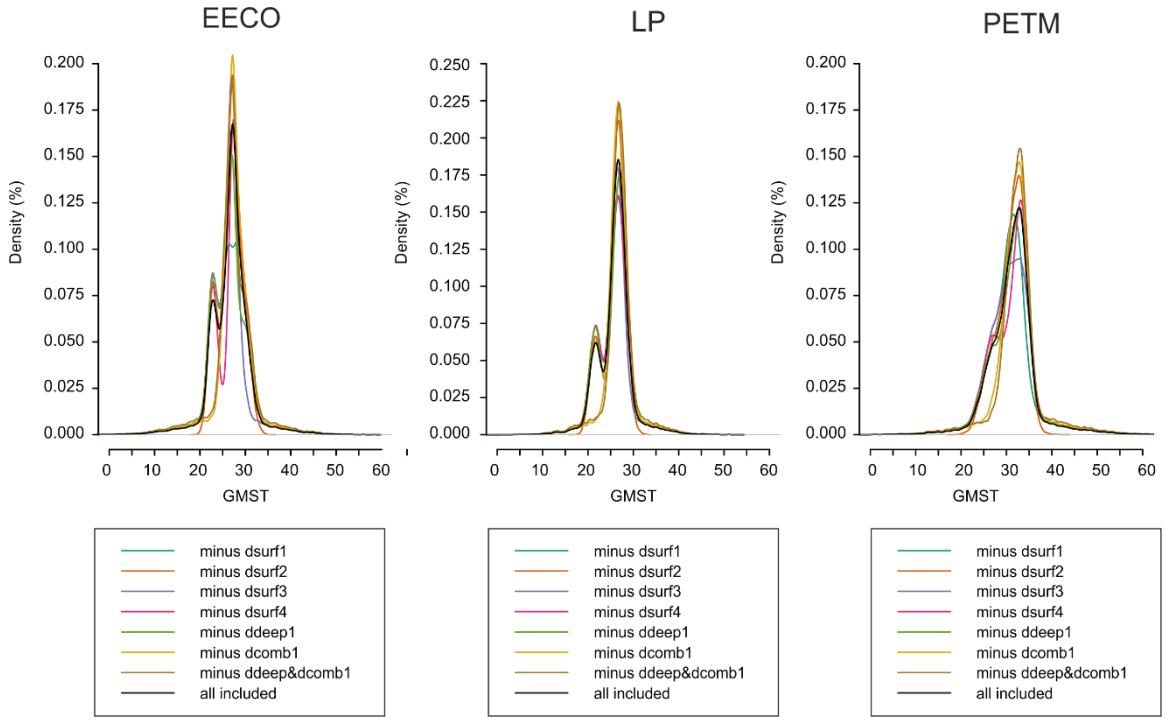

Supplementary Table 1. Summary of model simulations used to infer GMST

Model	Reference	Paleogeography	Sim. Length (years)	CO_2 levels
HadCM3L	Farnsworth et al (2019)	Getech	> 10,000	x2, 4
CESM1	Huber and Caballero (2011)	Sewall et al. (2000)	>3000	x4, 8, 16
CESM1.2	Zhu et al. (2019); Lunt et al. (2020)	Herold et al (2014)	> 2000	x3, 6, 9
GFDL	Hutchison et al. (2018); Lunt et al. (2020)	Herold et al (2014)	6000	x3, 6

Supplementary Table 2.

	LP	PETM	EECO	Primary references	Notes
DSDP 401	-	-	22	Nunes & Norris [2006]; Pak & Miller [1992]; Miller & Curry [1982]	Excluded from analysis (CIE <1.5‰)
DSDP 525	2	2	2	Shackleton *et al*. [1984]; Thomas & Shackleton [1996]	
DSDP 527	4	2		Thomas & Shackleton [1996]	
DSDP 549	-	-		Nunes & Norris [2006]	Excluded from analysis (see Dunkley-Jones *et al*. [2013])
DSDP 550			50	Charisi & Schmitz [1996]	
DSDP 577			20	Pak & Miller [1992]; Miller *et al*. [1987]	
ODP 690	67	6	5	Thomas & Shackleton [1996]; Stott *et al*. [1996]; Kennett & Stott [1990, 1991]; Kelly *et al*. [2005]; Thomas *et al*. [2002]; Nunes & Norris [2006]	
ODP 702			7	Katz & Miller [1991]	
ODP 738	5	3	16	Barrera & Huber [1991]; Lu & Keller [1993]	
ODP 865	-	-	14	Bralower *et al*. [1995]; Thomas *et al*. [2000]	Excluded from analysis (CIE <1.5‰)
ODP 1051	18	2		Katz *et al*. [2003]	
ODP 1209	32	9	491	Westerhold *et al*. [2011]; Westerhold *et al*. [2018]; Tripati & Elderfield [2005]	
ODP 1220	3	5		Nunes & Norris [2006]	
ODP 1258	3	3	140	Nunes & Norris [2006]; Sexton *et al*. [2011]	
ODP 1262	379	10	161	Barnet *et al*. [2019]; Lauretano *et al*. [2015]; Littler *et al*. [2014]; Stap *et al*. [2010]; McCarren *et al*. [2008]	
ODP 1263		6	900	Westerhold *et al*. [2018]; Lauretano *et al*. [2015]; Lauretano *et al*. [2018]; McCarren *et al*. [2008]	